

See discussions, stats, and author profiles for this publication at: <https://www.researchgate.net/publication/234070661>

# Isomerization Energy Decomposition Analysis for Highly Ionic Systems: Case Study of Starlike E<sub>5</sub>Li<sub>7</sub><sup>+</sup> Clusters

ARTICLE in CHEMISTRY - A EUROPEAN JOURNAL · FEBRUARY 2013

Impact Factor: 5.73 · DOI: 10.1002/chem.201203329 · Source: PubMed

CITATIONS

8

READS

23

8 AUTHORS, INCLUDING:



**Maryel Contreras**

Center for Research and Advanced Studies...

7 PUBLICATIONS 111 CITATIONS

SEE PROFILE



**Edison Humberto Osorio**

Fundación Universitaria Luis Amigó

23 PUBLICATIONS 92 CITATIONS

SEE PROFILE



**Franklin Ferraro**

Fundación Universitaria Luis Amigó

12 PUBLICATIONS 39 CITATIONS

SEE PROFILE



**William Tiznado**

Universidad Andrés Bello

55 PUBLICATIONS 637 CITATIONS

SEE PROFILE



# Isomerization Energy Decomposition Analysis for Highly Ionic Systems: Case Study of Starlike $E_5Li_7^+$ Clusters

Maryel Contreras,<sup>[a]</sup> Edison Osorio,<sup>\*,[b]</sup> Franklin Ferraro,<sup>[b]</sup> Gustavo Puga,<sup>[b]</sup> Kelling J. Donald,<sup>\*,[c]</sup> Jason G. Harrison,<sup>[d]</sup> Gabriel Merino,<sup>\*,[e]</sup> and William Tiznado<sup>\*,[b]</sup>

**Abstract:** The most stable forms of  $E_5Li_7^+$  ( $E = Ge, Sn, \text{ and } Pb$ ) have been explored by means of a stochastic search of their potential-energy surfaces by using the gradient embedded genetic algorithm (GEGA). The preferred isomer of the  $Ge_5Li_7^+$  ion is a slightly distorted analogue of the  $D_{5h}$  three-dimensional seven-pointed starlike structure adopted by the lighter  $C_5Li_7^+$  and  $Si_5Li_7^+$  clusters. In contrast, the preferred structures for  $Sn_5Li_7^+$

and  $Pb_5Li_7^+$  are quite different. By starting from the starlike arrangement, corresponding lowest-energy structures are generated by migration of one of the E atoms out of the plane with the a

corresponding rearrangement of the Li atoms. To understand these structural preferences, we propose a new energy decomposition analysis based on isomerizations (isomerization energy decomposition analysis (IEDA)), which enable us to extract energetic information from isomerization between structures, mainly from highly charged fragments.

**Keywords:** ab initio calculations • cluster compounds • isomerization energy decomposition analysis (IEDA) • isomerization • structural preferences

## Introduction

Silicon–lithium compounds became a popular topic of discussion after Cui and co-workers invented in 2008 the high-performance lithium battery anodes by using silicon nanowires.<sup>[1]</sup> They achieved a theoretical charge capacity for silicon anodes that is more than ten times higher than existing

graphite ones, allowing a far greater energy density on the anode, thus reducing the mass density ratio of the battery.<sup>[1–2]</sup> Recently, we explored the potential-energy surface of some small silicon–lithium clusters to gain some insight into the silicon–lithium aggregation process with a view to assessing how they interact with hydrogen molecules.<sup>[3]</sup> Clusters with the formula  $Si_5Li_n^{n-6}$  ( $n = 5–7$ ) are of particular interest to us because of their strong aromatic character, and when  $n = 7$ , the lowest energy form is a beautiful starlike structure<sup>[3d]</sup> (see also the related paper of Perez-Peralta and Boldyrev).<sup>[3c]</sup> More recently, we showed that the most stable configuration for  $C_5Li_7^+$  is a  $D_{5h}$  seven-pointed star.<sup>[4]</sup> Structures of  $Si_5Li_7^+$  and  $C_5Li_7^+$  can be described conceptually as ionic interactions of a flat  $E_5^{6-}$  pentagonal ring with seven satellite lithium cations. Interestingly, the  $Si_5^{6-}$  fragment is found in the solid state as a planar pentagon.<sup>[5]</sup> Further, Todorov, and Sevov found that flat  $Sn_5^{6-}$  and  $Pb_5^{6-}$  rings are also present in the Zintl phases  $Na_8BaPb_6$ ,  $Na_8BaSn_6$ , and  $Na_8EuSn_6$ .<sup>[6]</sup> These observations led us to examine the similarities and differences between the Ge, Sn, and Pb analogues of the C and Si systems described above. Due to differences in size and electronegativity among the Group 14 elements, lithium is expected to exhibit significant differences in its bonding interactions with the tin and lead anionic motif relative to silicon and carbon. Thus, we wanted to explore as thoroughly as possible the potential-energy surfaces of those heavier systems without pre-supposing that they would adopt the same starlike geometry in the gas phase as well.

By using high-level quantum chemical computation to extend our studies to the heavy  $E_5Li_7^+$  clusters (for  $E = Ge,$

- [a] M. Contreras  
Departamento de Química, Universidad de Guanajuato  
Noria Alta s/n 36050 Guanajuato (Mexico)
- [b] Dr. E. Osorio, F. Ferraro, G. Puga, Prof. W. Tiznado  
Departamento de Química, Facultad de Ciencias Exactas  
Universidad Andres Bello, Av. República 252, Santiago (Chile)  
Fax: (56-2) 661-8269  
E-mail: ed.osorio@uandresbello.edu  
wtiznado@unab.cl
- [c] Prof. K. J. Donald  
Department of Chemistry, Gottwaldov Center for the Sciences  
University of Richmond, Richmond, VA, 23173 (USA)  
Fax: (+1) 804-287-1897  
E-mail: kdonald@richmond.edu
- [d] J. G. Harrison  
Department of Chemistry, University of California, Davis  
Davis, CA 95616 (USA)
- [e] Prof. G. Merino  
Departamento de Física Aplicada  
Centro de Investigación y de Estudios Avanzados  
Unidad Mérida Km. 6 Antigua carretera a Progreso  
Apdo. Postal 73, Cordemex, 97310, Mérida, Yuc. (México)  
E-mail: gmerino@mda.cinvestav.mx

Supporting information for this article is available on the WWW under <http://dx.doi.org/10.1002/chem.201203329>.

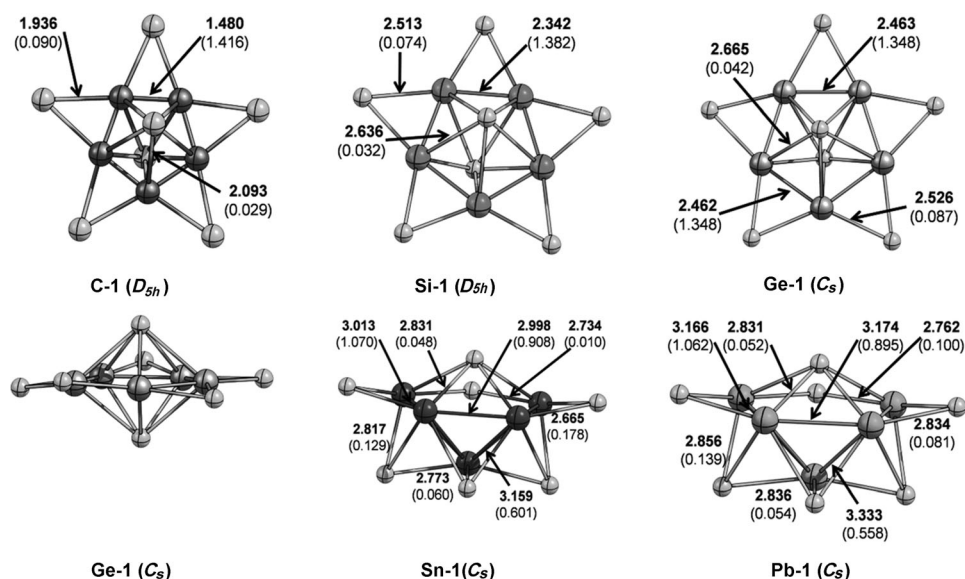


Figure 1. Global minimum structures for the  $E_5Li_7^+$  complexes ( $E = C, Si, Ge, Sn,$  and  $Pb$ ), with the relevant bond lengths [ $\text{\AA}$ ] given in bold and Wiberg bond indices given in parentheses.

$Sn, Pb$ ), we found that the most stable form of  $Ge_5Li_7^+$  is a slightly distorted  $D_{5h}$  structure, similar to those found for the  $C$  and  $Si$  cases (Figure 1). For  $Sn_5Li_7^+$  and  $Pb_5Li_7^+$ , however, the global minima are completely different. We examined what promoted these changes in the relative stabilities of the cluster isomers (from the starlike arrangement to an alternative based on a trapezoidal sub-structure) as a function of the  $E$  atoms going down Group 14. It is clear that the dominant contribution between the  $E_5$  ring and the alkali metal is ionic in nature, but the other bonding contributions can also be important. One option for obtaining more information about the bonding in these systems is energy decomposition analysis (EDA).<sup>[7]</sup> However, in ionic systems, the obvious fragments for EDA are multiply charged moieties, in our case  $E_5^{6-}$  and  $Li_6^{7+}$ , which possess strong intra-fragment Coulomb repulsion and are, therefore, extremely unstable. So, to analyze the bonding and the structural changes in these highly ionic clusters by using an energy-partitioning scheme, we employ in this work a new scheme to quantify the different contributions to the isomerization energy without the optimization of the fragments. Our isomerization energy decomposition analysis (IEDA) provides the ingredients required for a better understating of the isomerization process for any type of isomerization, especially in the case of highly ionic systems.

## Computational Methods

The potential-energy surfaces of the  $E_5Li_7^+$  ( $E = Ge, Sn,$  and  $Pb$ ) clusters were explored in detail by using the gradient-embedded genetic algorithm (GEGA).<sup>[8]</sup> We used the Perdew–Burke–Ernzerhof (PBE)<sup>[9]</sup> functional in conjunction with the SDD<sup>[10]</sup> basis sets for the energy, gradient, and force computations involved in the GEGA procedure. These computations were performed by using the Gaussian 03 suite of programs.<sup>[11]</sup>

The geometries obtained using the GEGA at the PBE/SDD model chemistry were reoptimized at the PBE/TZ2P. Uncontracted Slater-type orbitals (STO's) were employed as the basis functions for the self-consistent field (SCF) computations. The basis sets are of triple- $\zeta$  quality, augmented by two sets of polarization functions (TZ2P),<sup>[12]</sup> with  $d$  and  $f$  functions for all atoms. Harmonic frequency computations were performed to determine the nature of all stationary points. The scalar and the spin-orbit (SO) relativistic effects for  $Sn$  and  $Pb$  were incorporated by the zeroth order regular approximation (ZORA).<sup>[13]</sup> Shielding tensors were computed at the PBE/TZ2P and SAOP<sup>[14]</sup>/TZ2P levels by using the gauge-independent atomic orbital (GIAO) approximation.<sup>[15]</sup> These computations were performed by using the ADF2008.01 package.<sup>[16]</sup>

In the energy decomposition analysis (EDA), bond formation between the interacting fragments is divided into three steps, which can be interpreted in a plausible physically meaningful

way. In the first step, the fragments, which are computed with the frozen geometry of the entire molecule, are superimposed without electronic relaxation, yielding the quasiclassical electrostatic attraction  $\Delta V_{\text{elstat}}$ . In the second step the product wavefunction becomes antisymmetrized and re-normalized, which gives the repulsive term  $\Delta E_{\text{Pauli}}$ , termed Pauli repulsion. In the third step the molecular orbitals relax to their final form to yield the stabilizing orbital interaction  $\Delta E_{\text{oi}}$ . This final term can be divided into contributions of orbitals with different symmetries. The sum of the three terms  $\Delta E_{\text{Pauli}} + \Delta V_{\text{elstat}} + \Delta E_{\text{oi}}$  gives the total interaction energy  $\Delta E_{\text{int}}$  [Eq. (1)].

$$\Delta E_{\text{int}} = \Delta E_{\text{Pauli}} + \Delta V_{\text{elstat}} + \Delta E_{\text{oi}} \quad (1)$$

For chemical bonds or non-covalent contacts between monomeric or fragment units, the interaction energy,  $\Delta E_{\text{int}}$ , can be used to calculate the bond-dissociation energy,  $D_e$ , by adding  $\Delta E_{\text{prep}}$ , which is the necessary energy to promote the fragments from their equilibrium geometry to their geometry inside the compounds [Eq. (2)]. The advantage of using  $\Delta E_{\text{int}}$  instead of  $D_e$  is that the instantaneous electronic interaction of the fragments is analyzed, which yields a direct estimate of the energy components.

$$-D_e = \Delta E_{\text{prep}} + \Delta E_{\text{int}} \quad (2)$$

Finally, the natural population analysis (NPA) charges<sup>[17]</sup> and Wiberg bond indices (WBI)<sup>[18]</sup> were computed by using the PBE/def2-TZVPP//PBE/TZ2P<sup>[19]</sup> level in Gaussian 03.<sup>[11]</sup>

## Results and Discussion

**Structure and bonding:** Figure 1 shows the global minimum-energy structures for the  $E_5Li_7^+$  clusters, including  $C_5Li_7^+$  and  $Si_5Li_7^+$  for comparison.<sup>[20]</sup> The global minimum for  $Ge_5Li_7^+$  (**Ge-1** in Figure 1) is structurally similar to the  $C$  and  $Si$  molecular stars; however, the  $Ge_5$  ring is slightly distorted, with one of the  $Ge$  atoms out of plane with a dihedral angle of  $3.5^\circ$ . The dihedral angles formed by the equa-

torial Li atoms with the adjacent  $Ge_4$  trapezoid plane range from 6.0 to 7.0°, and the Ge–Ge bond lengths of 2.46 Å are in the range of a Ge–Ge single bond (2.42 Å). The energy difference between the  $D_{5h}$  structure and **Ge-1** is negligible (only 0.2 kcal mol<sup>−1</sup>), but the former has four small imaginary frequencies.

Our computations indicate that the strong preference for the starlike structure in the C and Si systems is partially lost for Ge and completely absent for the tin and lead clusters. The most stable  $Sn_5Li_7^+$  structure may be described as a trapezoidal  $Sn_5$  fragment (Figure 1), with 1) three of the triangular faces of the trapezium each capped by a Li atom, 2) a fourth Li atom capping the  $Sn_4$  base of the trapezium, 3) two Li atoms in bridging positions on the short sides of the trapezium, and 4) one Li atom bonding with two atoms of the longest side to form a flat  $Sn_4Li$  five-membered ring. This form is the global minimum, not only for  $Sn_5Li_7^+$ , but also for  $Pb_5Li_7^+$ .

Why is the  $D_{5h}$  starlike structure not even a minimum on the potential-energy surface for  $Sn_5Li_7^+$  and  $Pb_5Li_7^+$ ? The starlike structures are higher by 30 (Sn) and 25 kcal mol<sup>−1</sup> (Pb) in energy than the corresponding global minimum. The NPA performed on the global minima is summarized in Figure 1. For  $C_5Li_7^+$  and  $Si_5Li_7^+$ , the C–Li and Si–Li interactions are ionic in nature. And this is the case for the Ge system, as well. The  $Ge_5$  ring charge in **Ge-1** is −5.40 versus −5.30 and −5.40 e<sup>−</sup> for the carbon and silicon analogues, respectively. This Ge system may also be viewed as a very negatively charged  $E_5^{6-}$  ring interacting with a  $Li_7^{7+}$  moiety. In **Sn-1** and **Pb-1**, the interaction between the  $E_5$  fragment and the lithium atoms is also ionic. The negative charges of the  $E_5$  fragments are slightly lower than in the starlike structures, but remain very high (−4.91 and −4.84 e<sup>−</sup> in **Sn-1** and **Pb-1**, respectively).

The E–E WBI's in the starlike structures are 1.42, 1.38, 1.35, 1.33, and 1.31 for **C-1**, **Si-1**, **Ge-1**,  $Sn_5Li_7^+$  ( $D_{5h}$ ), and  $Pb_5Li_7^+$  ( $D_{5h}$ ), respectively. In contrast, the WBI values for the tin and lead global minima are between 1.07 and 0.86. For the E atom that is outside the trapezoidal fragment (see Figure 1), the bond order is a bit lower (WBI=0.6), which suggests that there is a smaller covalent contribution to that bond. In all the systems, the E–Li WBI values are extremely small (ranging from 0.01–0.10), which is in agreement with the inference that the clusters are substantially ionic, at least in regard to the Li–E interactions. The atomic charges also indicate the ionic character of the E–Li interactions in all the  $E_5Li_7^+$  clusters. All of this information, while interesting and useful, unfortunately still gives no concrete insight into the nature of the structural preferences in the systems. What is more noteworthy is that the  $z$ -component of the induced magnetic field<sup>[21]</sup> (equivalent to  $NICS_{zz}$ <sup>[22]</sup>) shows that in all cases its starlike isomers have a strong diatropic response, that is, these systems could be considered to be aromatic.<sup>[23]</sup>

**Energy decomposition analysis:** Traditional decomposition analysis schemes have been quite useful in aiding computational chemists in resolving various complex chemical ques-

Table 1. Results of EDA at the PBE/TZ2P level for  $E_5Li_7^+$  with  $E_5^{6-} + Li_7^{7+}$  as fragments.  $\Delta E_{iso}$  is the isomerization energy with respect to the starlike form. Energy values are in kcal mol<sup>−1</sup>.

		$\Delta E_{int}$	$\Delta E_{oi}$	$\Delta V_{elstat}$	$\Delta E_{Pauli}$	$\Delta E_{iso}$
$C_5Li_7^+$	$D_{5h}$	−4743.4	−307.2	−4830.1	393.8	–
	$C_s$	−4835.0	−374.2	−4789.8	328.3	92.0
$Si_5Li_7^+$	$D_{5h}$	−3606.1	−397.4	−3428.1	219.4	–
	$C_s$	−3731.2	−498.5	−3444.6	211.9	9.6
$Ge_5Li_7^+$	$D_{5h}$	−3514.9	−495.6	−3229.9	210.6	–
	$C_s$	−3655.2	−745.4	−3095.9	186.1	7.3
$Sn_5Li_7^+$	$D_{5h}$	−3279.0	−487.8	−2960.5	169.3	–
	$C_s$	−3459.4	−731.4	−2899.4	171.4	−7.2
$Pb_5Li_7^+$	$D_{5h}$	−3214.6	−438.3	−2944.5	168.2	–
	$C_s$	−3373.6	−612.4	−2928.9	167.7	−19.1

tions.<sup>[24]</sup> We started our analysis by decomposing the interaction energy of each isomer into the traditional Pauli ( $\Delta E_{Pauli}$ ), orbital interaction ( $\Delta E_{oi}$ ), and electrostatic contributions ( $\Delta V_{elstat}$ ; see Table 1). As in any partitioning-energy scheme, the main issue is defining the right fragments. The cluster, of course, does not care; it will make any electron shift to maximize bonding. Let us consider then the  $E_5^{6-}$  and  $Li_7^{7+}$  units as appropriate fragments to analyze the E–Li interactions and to understand the stability of the trapezoid structure in the Sn and Pb clusters. The interaction energy term is stronger in the  $C_s$  isomer for all the clusters, but that does not explain the energy differences between the isomers, and the individual components do not yield any apparent trends either.

For those reasons, we considered that it would be logical and clearer to explain the isomerization energy in terms of the change between the energy contributions on going from one isomer to the other ( $\Delta\Delta E_x = \Delta E_{x(E_5Li_7^+(C_s))} - \Delta E_{x(E_5Li_7^+(D_{5h}))}$ ). In general, the differences between the Pauli energy contributions ( $\Delta\Delta E_{Pauli}$ ) are close to zero (see Table 2). That

Table 2. Relative energy differences at the PBE/TZ2P level for the  $E_5Li_7^+$  clusters with  $E_5^{6-} + Li_7^{7+}$  as fragments. Energy values are in kcal mol<sup>−1</sup>.

	$\Delta\Delta E_{Pauli}$	$\Delta\Delta V_{elstat}$	$\Delta\Delta E_{oi}$	$\Delta\Delta E_{int}$
C	65.5	−40.3	67.0	92.2
Si	7.5	16.5	101.1	125.1
Ge	24.4	−134.0	249.8	140.2
Sn	−2.1	−61.1	243.6	180.4
Pb	0.5	−15.6	174.2	159.1

is the individual  $\Delta E_{Pauli}$  values are quite similar for each isomer. The differences in the electrostatic contributions ( $\Delta\Delta V_{elstat}$ ) are negative, except for the Si cluster, which indicates that the contribution of the trapezium to the  $\Delta\Delta V_{elstat}$  is dominant. In contrast, the orbital contribution ( $\Delta\Delta E_{oi}$ ) for every cluster is positive. So, the more dominant contribution to  $\Delta\Delta E_{oi}$  comes from the starlike isomer.

This data shows that traditional EDA does not lead us to a satisfactory understanding of the relative stability of the  $E_5Li_7^+$  isomers, and neither does it provide much insight into the isomeric preferences of these species. For this

reason we designed a new strategy for analyzing the electronic energy contributions to the (in)stability of our cluster systems.

**Isomerization energy decomposition analysis:** How to explain the preference for the lower symmetry cluster geometry for  $E = \text{Sn}$  and  $\text{Pb}$  (Figure 1)? To gain some quantitative insight into the nature of the  $E\text{-Li}$  interaction in  $E_5\text{Li}_7^+$ , and how this contributes to the stabilization of starlike or trapezoidal structures, we considered the hypothetical reaction cycle shown in Figure 2. The horizontal reactions corre-

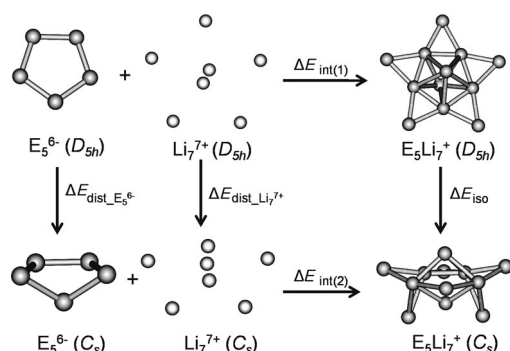


Figure 2. Energetic reaction cycle involving the isomerization of the  $E_5\text{Li}_7^+$  between  $D_{5h}$  and  $C_s$  structures.

spond to the interactions between the isolated  $E_5^{6-}$  and  $\text{Li}_7^{7+}$  fragments to form the  $D_{5h}$  and  $C_s$  isomers, whereas the vertical reactions involve the fragment distortion.

The changes in energy associated with each transformation have been estimated by Equations (3–9) and the results are reported in Table 3. This reaction cycle gives us a means

Table 3. Results of IEDA at the PBE/TZ2P level for the  $E_5\text{Li}_7^+$  clusters with  $E_5^{6-} + \text{Li}_7^{7+}$  as fragments. Energy values are in  $\text{kcal mol}^{-1}$ .

	$\Delta E_{\text{iso}}$	$\Delta E_{\text{int}(1)}$	$\Delta E_{\text{int}(2)}$	$\Delta E_{\text{dist}, E_5^{6-}}$	$\Delta E_{\text{dist}, \text{Li}_7^{7+}}$	$\Delta E_{\text{dist}}$	$\Delta\Delta E_{\text{int}}$
C	92.0	−4743.4	−4835.7	129.3	54.8	184.1	−92.3
Si	9.6	−3606.1	−3731.2	35.7	98.8	134.5	−125.1
G	7.3	−3514.9	−3655.2	8.7	138.6	147.3	−140.3
Sn	−7.2	−3279.0	−3459.4	10.5	162.3	172.7	−180.4
Pb	−19.1	−3214.6	−3373.6	−8.5	148.4	140.0	−159.0

to decompose the isomerization energy into two terms: the distortion energy ( $\Delta E_{\text{dis}}$ ) and the interaction energy difference ( $\Delta\Delta E_{\text{int}}$ ), which when combined with each other gives us an estimate of the energy of isomerization ( $\Delta E_{\text{iso}}$ ).

$$\Delta E_{\text{int}(1)} = E_{E_5\text{Li}_7^+(D_{5h})} - [E_{E_5^{6-}(D_{5h})} + E_{\text{Li}_7^{7+}(D_{5h})}] \quad (3)$$

$$\Delta E_{\text{int}(2)} = E_{E_5\text{Li}_7^+(C_s)} - [E_{E_5^{6-}(C_s)} + E_{\text{Li}_7^{7+}(C_s)}] \quad (4)$$

$$\Delta E_{\text{dist}, E_5^{6-}} = E_{E_5^{6-}(C_s)} - E_{E_5^{6-}(D_{5h})} \quad (5)$$

$$\Delta E_{\text{dist}, \text{Li}_7^{7+}} = E_{\text{Li}_7^{7+}(C_s)} - E_{\text{Li}_7^{7+}(D_{5h})} \quad (6)$$

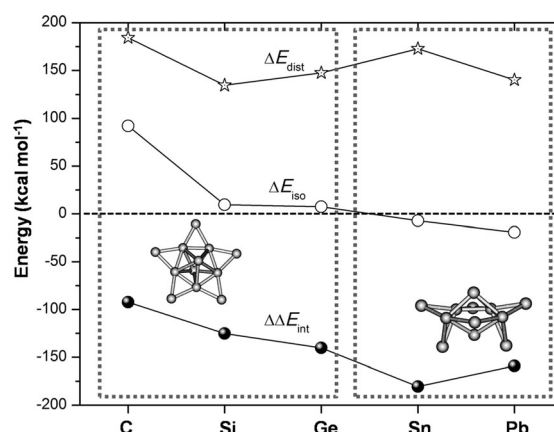


Figure 3. Contributions to the isomerization energy for the  $E_5\text{Li}_7^+$  clusters from Equations (1–7) by using IEDA.

$$\Delta E_{\text{dist}} = \Delta E_{\text{dist}, E_5^{6-}} + \Delta E_{\text{dist}, \text{Li}_7^{7+}} \quad (7)$$

$$\Delta\Delta E_{\text{int}} = \Delta E_{\text{int}(2)} - \Delta E_{\text{int}(1)} \quad (8)$$

$$\Delta E_{\text{iso}} = E_{E_5\text{Li}_7^+(C_s)} - E_{E_5\text{Li}_7^+(D_{5h})} = \Delta\Delta E_{\text{int}} + \Delta E_{\text{dist}} \quad (9)$$

To be able to say which geometry is preferred ( $C_s$  or  $D_{5h}$ ), the quantitative relationship between distortion and interaction energies ( $\Delta E_{\text{dist}}$ ) in the IEDA must be known. The two contributions to  $\Delta E_{\text{iso}}$  are depicted in Figure 3. From this data, it becomes apparent that the interaction energy is stronger in the trapezoidal form for all the clusters, but in the case of  $C_5\text{Li}_7^+$ , the energy involved in the structural changes ( $\Delta E_{\text{dist}}$ ) is almost twice the absolute value of  $\Delta\Delta E_{\text{int}}$ . So the main reason that the isomer with the trapezoidal substructure is not competitive for the carbon cluster is that the geometrical changes from the star to the trapezoid are exceptionally expensive, with the carbon fragment being the most reluctant to change (with  $\Delta E_{\text{dist}, E_5^{6-}} = 129.3 \text{ kcal mol}^{-1}$ , Table 3). In the case of the Si and Ge systems,  $\Delta E_{\text{dist}}$  is only moderately higher than the absolute value of  $\Delta\Delta E_{\text{int}}$ . Indeed, the  $E_5^{6-}$  skeleton is quite flexible in the sense that it only needs 35.2 (Si) and 8.7  $\text{kcal mol}^{-1}$  (Ge) to change from the planar to the trapezoidal form. In contrast, the  $\Delta E_{\text{dist}, \text{Li}_7^{7+}}$  value increases gradually from C to Sn. In the case of the heavier Sn and Pb analogues, the  $\Delta E_{\text{dist}}$  is considerable, but the large  $\Delta E_{\text{dist}}$  values for  $E = \text{Sn}$  and  $\text{Pb}$  are outstripped by an increase of the interaction in the trapezoid isomers.

These results enable us to rationalize the origins of the isomeric preferences in these highly ionic clusters in a quantitative way, by using our new IEDA approach. The conventional EDA approach fails to properly account for these preferences because it is hard to compute the corresponding preparation energy; however, the IEDA method provided us with a straightforward way to think about the relative stability of the heavier cationic  $E_5\text{Li}_7^+$  clusters. Now, although this IEDA formulation was developed to handle these series of complex situations, it is applicable much more broadly to any type of isomerization analysis, especially in the cases of



highly ionic systems that are not well suited to classical approaches in which distinct ionic fragments can be readily identified.

## Conclusion

Our systematic exploration of the potential-energy surfaces of the  $E_5Li_7^+$  ( $E = Ge, Sn, \text{ and } Pb$ ) systems demonstrates that the global minimum structure of  $Ge_5Li_7^+$  resembles a distorted starlike form, whereas the global minima for the  $Sn_5Li_7^+$  and  $Pb_5Li_7^+$  structures are completely different. We examined the cause of this significant break in the relative stabilities of the cluster going down Group 14 by using a novel IEDA approach and found that the interaction energies are stronger in the trapezoidal form for all the clusters. However, the energy involved in the structural changes going from the  $D_{5h}$  to the  $C_s$  isomer structures ( $\Delta E_{\text{dist}}$ ) is positive. Both terms are competitive for the E atoms below C in Group 14 of the periodic table (Figure 3), but in the case of the Sn and Pb clusters the energy required for the structural changes, from the star to the trapezoidal form, is somewhat smaller than the magnitude of the relative interaction energy. For this reason, the  $C_s$  structure is competitive for the tin and the lead clusters.

From this analysis, we have found, indeed, that the newly developed IEDA approach provides qualitative insight, based on accurate calculations, into the origin of isomerization reactions. In this model, the isomerization energy is decomposed into the relative change of the distortion energies ( $\Delta E_{\text{dist}}$ ) plus the difference in the interaction energies ( $\Delta \Delta E_{\text{int}}$ ), so  $\Delta E_{\text{iso}} = \Delta E_{\text{dist}} + \Delta \Delta E_{\text{int}}$ . The distortion energy term is directly related to the fragment's capacity to transform one isomer into the other. The interaction term reflects the bonding capabilities of each isomer. The insights that emerge from the IEDA calculations have enabled us to interpret and rationalize our computational findings in a relatively straightforward way.

## Acknowledgements

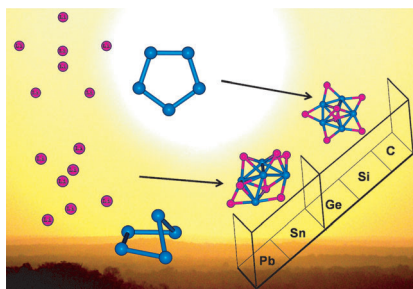
The authors acknowledge the General Coordination of Information and Communication Technologies (CGSTIC) at CINVESTAV for providing HPC resources on the Hybrid Cluster Supercomputer "Xihucatl". W.T. acknowledges Fondecyt for funding under grant no. 11090431. At the University of Richmond, K.J.D. gratefully acknowledges the National Science Foundation for funding under NSF-CAREER CHE-1056430. M.C. acknowledges Conacyt for the PhD fellowship.

- [1] C. K. Chan, H. L. Peng, G. Liu, K. McIlwrath, X. F. Zhang, R. A. Huggins, Y. Cui, *Nat. Nanotechnol.* **2008**, *3*, 31–35.
- [2] L. F. Cui, R. Ruffo, C. K. Chan, H. L. Peng, Y. Cui, *Nano Lett.* **2009**, *9*, 491–495.
- [3] a) E. Osorio, V. Villalobos, J. C. Santos, K. J. Donald, G. Merino, W. Tiznado, *Chem. Phys. Lett.* **2012**, *522*, 67–71; b) S. Pan, G. Merino, P. K. Chattaraj, *Phys. Chem. Chem. Phys.* **2012**, *14*, 10345–10350; c) J. C. Santos, M. Contreras, G. Merino, *Chem. Phys. Lett.* **2010**, *496*, 172–174; d) W. Tiznado, N. Perez-Peralta, R. Islas, A. Toro-
- Labbe, J. M. Ugalde, G. Merino, *J. Am. Chem. Soc.* **2009**, *131*, 9426–9431; e) N. Perez-Peralta, A. I. Boldyrev, *J. Phys. Chem. A* **2011**, *115*, 11551–11558.
- [4] N. Perez-Peralta, M. Contreras, W. Tiznado, J. Stewart, K. J. Donald, G. Merino, *Phys. Chem. Chem. Phys.* **2011**, *13*, 12975–12980.
- [5] a) A. Kuhn, P. Sreeraj, R. Pöttgen, H.-D. Wiemhöfer, M. Wilkening, P. Heitjans, *Angew. Chem.* **2011**, *123*, 12305–12308; *Angew. Chem. Int. Ed.* **2011**, *50*, 12099–12102; b) R. Nesper, J. Curda, H. G. Von Schnering, *J. Solid State Chem.* **1986**, *62*, 199–206.
- [6] I. Todorov, S. C. Sevov, *Inorg. Chem.* **2004**, *43*, 6490–6494.
- [7] a) K. Morokuma, *J. Chem. Phys.* **1971**, *55*, 1236–1244; b) T. Ziegler, A. Rauk, *Theor. Chim. Acta* **1977**, *46*, 1–10; c) A. Diefenbach, F. M. Bickelhaupt, G. Frenking, *J. Am. Chem. Soc.* **2000**, *122*, 6449–6458; d) M. von Hopffgarten, G. Frenking, *WIREs Comput. Mol. Sci.* **2012**, *2*, 43–62.
- [8] a) A. N. Alexandrova, A. I. Boldyrev, *J. Chem. Theory Comput.* **2005**, *1*, 566–580; b) A. N. Alexandrova, A. I. Boldyrev, Y. J. Fu, X. Yang, X. B. Wang, L. S. Wang, *J. Chem. Phys.* **2004**, *121*, 5709–5719.
- [9] a) J. P. Perdew, K. Burke, M. Ernzerhof, *Phys. Rev. Lett.* **1996**, *77*, 3865–3868; b) J. P. Perdew, K. Burke, M. Ernzerhof, *Phys. Rev. Lett.* **1997**, *78*, 1396–1396.
- [10] a) P. Fuentealba, H. Preuss, H. Stoll, L. v. Szentpály, *Chem. Phys. Lett.* **1982**, *89*, 418–422; b) G. Igel-Mann, H. Stoll, H. Preuss, *Mol. Phys.* **1988**, *65*, 1321–1328.
- [11] Gaussian 03, Revision B03, M. J. Frisch, G. W. Trucks, H. B. Schlegel, G. E. Scuseria, M. A. Robb, J. R. Cheeseman, J. A. Montgomery, Jr., T. Vreven, K. N. Kudin, J. C. Burant, J. M. Millam, S. S. Iyengar, J. Tomasi, V. Barone, B. Mennucci, M. Cossi, G. Scalmani, N. Rega, G. A. Petersson, H. Nakatsuji, M. Hada, M. Ehara, K. Toyota, R. Fukuda, J. Hasegawa, M. Ishida, T. Nakajima, Y. Honda, O. Kitao, H. Nakai, M. Klene, X. Li, J. E. Knox, H. P. Hratchian, J. B. Cross, V. Bakken, C. Adamo, J. Jaramillo, R. Gomperts, R. E. Stratmann, O. Yazyev, A. J. Austin, R. Cammi, C. Pomelli, J. W. Ochterski, P. Y. Ayala, K. Morokuma, G. A. Voth, P. Salvador, J. J. Dannenberg, V. G. Zakrzewski, S. Dapprich, A. D. Daniels, M. C. Strain, O. Farkas, D. K. Malick, A. D. Rabuck, K. Raghavachari, J. B. Foresman, J. V. Ortiz, Q. Cui, A. G. Baboul, S. Clifford, J. Cioslowski, B. B. Stefanov, G. Liu, A. Liashenko, P. Piskorz, I. Komaromi, R. L. Martin, D. J. Fox, T. Keith, M. A. Al-Laham, C. Y. Peng, A. Nanayakkara, M. Challacombe, P. M. W. Gill, B. Johnson, W. Chen, M. W. Wong, C. Gonzalez, J. A. Pople, Gaussian, Inc., Wallingford CT, **2004**.
- [12] E. van Lenthe, E. J. Baerends, *J. Comput. Chem.* **2003**, *24*, 1142–1156.
- [13] a) E. van Lenthe, A. Ehlers, E. J. Baerends, *J. Chem. Phys.* **1999**, *110*, 8943–8953; b) E. van Lenthe, E. J. Baerends, J. G. Snijders, *J. Chem. Phys.* **1994**, *101*, 9783–9792.
- [14] a) O. V. Gritsenko, P. R. T. Schipper, E. J. Baerends, *Chem. Phys. Lett.* **1999**, *302*, 199–207; b) P. R. T. Schipper, O. V. Gritsenko, S. J. A. v. Gisbergen, E. J. Baerends, *J. Chem. Phys.* **2000**, *112*, 1344–1352.
- [15] a) G. Schreckenbach, T. Ziegler, *J. Phys. Chem.* **1995**, *99*, 606–611; b) S. K. Wolff, T. Ziegler, *J. Chem. Phys.* **1998**, *109*, 895–905.
- [16] E. J. Baerends, *ADF2008.01, Scientific Computing and Modelling NV*, Theoretical Chemistry, Vrije Universiteit, Amsterdam, **2008**.
- [17] A. E. Reed, R. B. Weinstock, F. Weinhold, *J. Chem. Phys.* **1985**, *83*, 735–746.
- [18] K. A. Wiberg, *Tetrahedron* **1968**, *24*, 1083–1096.
- [19] F. Weigend, R. Ahlrichs, *Phys. Chem. Chem. Phys.* **2005**, *7*, 3297–3305.
- [20] The higher-energy isomers at least 10 kcal mol<sup>−1</sup> above the global minima can be found in the Supporting Information.
- [21] a) T. Heine, R. Islas, G. Merino, *J. Comput. Chem.* **2007**, *28*, 302–309; b) G. Merino, T. Heine, G. Seifert, *Chem. Eur. J.* **2004**, *10*, 4367–4371; c) R. Islas, T. Heine, G. Merino, *Acc. Chem. Res.* **2012**, *45*, 215–228.
- [22] a) Z. F. Chen, C. S. Wannere, C. Corminboeuf, R. Puchta, P. v. R. Schleyer, *Chem. Rev.* **2005**, *105*, 3842–3888; b) C. Corminboeuf, T. Heine, G. Seifert, P. v. Schleyer, J. Weber, *Phys. Chem. Chem. Phys.*

- 2004, 6, 273–276; c) H. Fallah-Bagher-Shaidaei, C. S. Wannere, C. Corminboeuf, R. Puchta, P. v. Schleyer, *Org. Lett.* **2006**, 8, 863–866.
- [23] a)  $B_{\text{e}}^{\text{ind}}$  profiles of the  $\text{E}_5\text{Li}_7^+$  ( $D_{5h}$ ) clusters calculated at the SAOP/TZ2P levels by using the GIAO approximation and including spin-orbit (SO) relativistic effects are reported in Figure S4 of the Supporting Information; b) A. C. Castro, E. Osorio, J. O. C. Jimenez-Halla, E. Matito, W. Tiznado, G. Merino, *J. Chem. Theory Comput.* **2010**, 6, 2701–2705.
- [24] a) F. M. Bickelhaupt, E. J. Baerends, *Rev. Comput. Chem.* **2000**, 15, 1–86; b) A. Krapp, F. M. Bickelhaupt, G. Frenking, *Chem. Eur. J.* **2006**, 12, 9196–9216.

Received: September 17, 2012  
Published online: ■■■, 0000

**Structural analysis:** Combination of lithium and Group 14 elements are shown to prefer one of two distinct  $E_5Li_7^+$  clusters ( $E = C, Si, Ge, Sn,$  and  $Pb$ ) depending on the identity of  $E$ , and the preferences are rationalized on the basis of a simple isomerization energy decomposition scheme (see figure).



### Ab Initio Calculations

*M. Contreras, E. Osorio,\* F. Ferraro, G. Puga, K. J. Donald,\* J. G. Harrison, G. Merino,\* W. Tiznado\* ..... ■■■–■■■*

**Isomerization Energy Decomposition Analysis for Highly Ionic Systems: Case Study of Starlike  $E_5Li_7^+$  Clusters**

